

Characterizing spatiotemporal dynamics of land cover with multi-temporal remotely sensed imagery in Beijing during 1978–2010

Jinling Zhao · Wei Guo · Wenjiang Huang · Linsheng Huang · Dongyan Zhang · Hao Yang · Lin Yuan

Received: 28 December 2012 / Accepted: 7 August 2013
© Saudi Society for Geosciences 2013

Abstract To facilitate urban planning and management in fast-growing metropolitan areas, it is highly necessary to detect the spatiotemporal changes of different land cover types. This study aimed at identifying Beijing's land cover types and detecting the characteristics of their spatiotemporal changes using time series remote sensing and GIS techniques from 1978 to 2010. A total of 16 Landsat MSS/TM/ETM+ images were collected during the spring and late summer seasons. After preprocessing the dataset, artificial neural network was used to perform the land cover classification. Consequently, four maps were generated for 1978, 1992, 2000, and 2010, with six classes (agriculture, woodland, grassland, water, urban, and barren land) according to the level I classification scheme. Three transition matrices were constructed to represent all possible changes that occur in the landscape. The results showed that agriculture, barren land, and grassland had an increase in area, while urban, water, and woodland had a reduction within the study area. A total of 2,032.341 km² agriculture was reduced and 2,359.146 km² woodland was increased. In the three periods for 1978–1992, 1992–2000, 2000–2010, agriculture had the largest amount of transfer out primarily to urban class around central urban areas

and woodland had the most transfer in mainly from barren land in mountainous areas. More importantly, the driving forces analysis including economic development, growth of population and construction areas, and institutional policies was conducted to find out the primary factors inducing the land cover change.

Keywords Land cover · Landsat imagery · Remote sensing · Change detection · Driving forces analysis

Introduction

Land is one of the most valuable natural resources for human beings, which plays a pivotal role in human settlements, food supply, economic, social and political activities, etc. As a crucial carrier of various biophysical categories in the earth, its surface is covered by different natural vegetation and man-made features, such as vegetation regions (trees, bushes, lawns, etc.), bare soil, hard surfaces (rocks, buildings, etc.) and wet areas and bodies of water (sheets of water and watercourses, wetlands, etc.) (Lambin and Strahler 1994). Furthermore, natural resource management, climate change, planning and monitoring programs greatly depend on the accurate information from land cover at a given spatial scale: local, regional, or global (Lambin et al. 2003; Feddema et al. 2005; Youssef et al. 2011). At the same time, land cover change stemming from human land uses represents a major source and a major element of global environmental change (Turner II et al. 1994). Different land cover types were found to markedly affect the land use changes, so reliable information on land use/land cover, especially at a global scale, is required to assist in the solution of a wide range of environmental problems (Flamenco-Sandoval et al. 2007; Tehrany et al. 2013; Biro et al. 2013). Nevertheless, the land cover landscapes have been suffering from rapid changes due to severe human-related activities over the past dozens of years (Ramankutty

J. Zhao · L. Huang · D. Zhang
Key Laboratory of Intelligent Computing and Signal Processing,
Ministry of Education, Anhui University, Hefei 230039, China

W. Guo
College of Information and Management Science,
Henan Agriculture University, Zhengzhou 450002, China

W. Huang (✉)
Institute of Remote Sensing and Digital Earth,
Chinese Academy of Sciences, Beijing 100094, China
e-mail: yellowstar0618@163.com

H. Yang · L. Yuan
Beijing Research Center for Information Technology in Agriculture,
Beijing Academy of Agriculture and Forestry Sciences,
Beijing 100097, China

and Foley 1999; Al-shalabi et al. 2012; Matinfar et al. 2013). Consequently, it is quite important to make sure that they can be used rationally under a long-term strategic management. To recognize and manage the land resources, it is of great importance to quickly identify and dynamically monitor the land cover, especially at a large spatial scale and over long time spans.

In practice, there are two primary methods to capture information on land cover: field survey and remote sensing-based analysis. Land cover information from conventional ground-based data has significant deficiencies. For instance, they are always acquired by statistical analysis from specific sampling points and cannot represent the entire study area well. It will also inevitably be a time-consuming and costly process with low efficiency, especially at large spatial scales. Conversely, the rapid development and advancement of remote sensing technology provides an effective tool for monitoring land cover at global, continental, regional, and local scales (Sobrino and Raissouni 2000). In comparison with traditional ground-based land cover maps, maps produced from optical satellite data have advantages in spatial expansion and statistical analysis, due to the continuous coverage and internal consistency (DeFries and Townshend 1994). Since the successful launch of the first satellite in the Landsat satellite series in 1972, thousands of images from the Multispectral Scanner (MSS), the Thematic Mapper (TM), and the Enhanced Thematic Mapper Plus (ETM+) have been extensively and successfully used in the identification of land use/land cover information (Haack et al. 1987; Rogan et al. 2003; Stathopoulou and Cartalis 2007). Over the past years, different types of remote sensing data have been widely used to identify land cover information. Stone et al. (1994) have developed a map of the land cover of South America based largely on multi-temporal National Oceanic and Atmospheric Administration (NOAA) Advanced Very High Resolution Radiometer (AVHRR) LAC (Local Area Coverage) 1-km resolution data. Loveland et al. (2000) have produced a 1-km resolution global land cover layer, named the IGBP DISCover Product from the AVHRR dataset. Kelarestaghi and Jeloudar (2011) detected the land use and cover change of the Lajimrood Drainage Basin in northern parts of Iran, based on 1:25,000 digital topographic maps dated 1967 and 1994 and etM+ satellite image dated 2002. In the previous studies based on remote sensing imagery, there are usually two problems confronting the land cover: (1) how to select appropriate remote sensing imagery and (2) how to obtain more accurate identification accuracy.

With the fast development of social and economic activities, how to quickly monitor the land cover changes has been paid special attention, especially in rapidly growing metropolitan areas. Land cover and its change have a significant impact on rational and sustainable planning for regional resource development, especially for the metropolitan areas with fast-

developing socioeconomic and human activities (Al-shalabi et al. 2013). Beijing, as the capital of the People's Republic of China, is the country's political, cultural, and educational center. Its land cover categories are undergoing significant changes, such as urban sprawl, forestry and agricultural land reduction, etc. The importance of accurate and timely information describing the nature and extent of land resources and the corresponding changes over time is increasing. However, it is always difficult to obtain the land cover and its change features of Beijing using traditional statistical method. In comparison with some low-resolution optical satellite data (e.g., MODIS, NOAA/AVHRR), longer time span, wider swath coverage, and higher spatial resolution make Landsat imagery sufficient and reliable to be used in the characterization of land use/land cover dynamic changes of Beijing.

In this study, a total of 16 Landsat MSS/TM/ETM+ images were collected, which were mainly located during the spring and late summer seasons. After performing the data preprocessing, artificial neural network (ANN) was used to perform land cover classification by integrating different kinds of remotely sensed data and their derivatives. The specific objectives of this study were to (1) identify the land cover types and dynamically monitor their spatiotemporal changes during 1978–2010, based on the Landsat time series imagery and other ancillary data, and (2) more importantly, driving forces analysis was performed to find out the primary influence factors. This study can provide a methodological reference for rationally performing the planning and management of land resources at multiple spatial and temporal scales, especially in diversely changing metropolitan areas.

Materials and methods

The area selected for this study is Beijing Metropolis located between 115°25' and 117°30' in longitudes and 39°26' and 41°03' in latitudes, which includes a diversity of land cover types (Fig. 1). The topography is composed of mountains to the north, northwest, and west and plain areas to the southeast. There is a total land area of approximately 16,000 km² in this study area, among which mountainous areas account for 61.4 % and plain areas account for 38.6 %. It is administratively divided by 14 urban and suburban districts and 2 rural counties. Beijing has a monsoon-influenced humid continental climate, with an annual average temperature of 10–12 °C and an annual average rainfall of more than 600 mm.

Selection of Landsat time series imagery

In general, different land cover types usually have specific phenologies, especially for green plants. However, it is still inevitable that mixed types are identified due to similar spectra or textures among different types. Consequently, it is quite

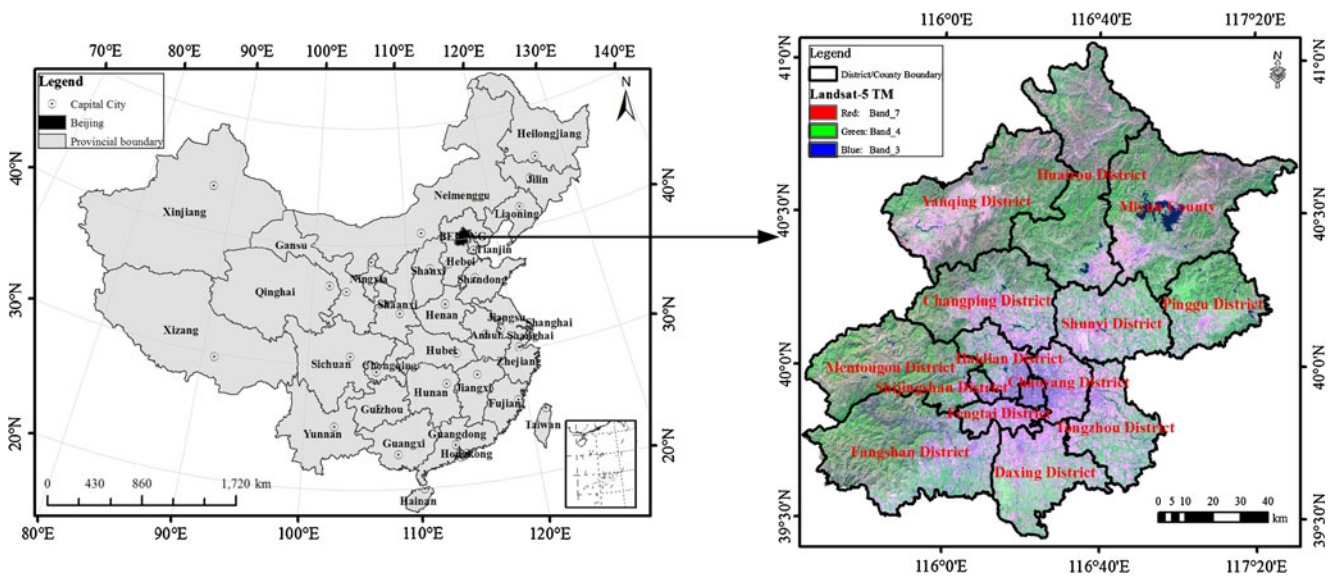


Fig. 1 Geographical location of the study area

necessary that temporal differences need to be used for identifying pure types in accordance with their specific features. In comparison with single temporal image, both the average and the minimum separability of different types can be increased by combining spring and summer images (Yuan et al. 2005). Furthermore, multi-temporal images can also detect change information for a certain type in specific time interval. In the spring image, annual crops (e.g., soybean and maize) are planted in the fields covered with bare soil, which can be obviously distinguishable from forests that are already fully leafed out at that time. Conversely, forests and some crops are indistinguishable in the summer image due to their spectral similarity. Nevertheless, those same croplands from urban areas with significant amounts of asphalt and concrete and other impervious surfaces that are spectrally similar to bare soil in the spring image, so the late summer image has to be required (Yuan et al. 2005)

The Landsat Program is the longest running exercise in the collection of multi-temporal, multi-spectral, and multi-resolution range of imagery appropriate for land cover analysis. Landsat imagery has been available since 1972 from six satellites, with three primary sensors evolving over 30 years: MSS, TM, and etM+. To identify and map land use/land cover more accurately, multi-temporal imagery have been shown to be valuable and indispensable (Oettera et al. 2000). Two scenes have to be required to cover the entire study area: paths 132 and 133, row 32 for Landsat MSS sensor and path 123, rows 32 and 33 for Landsat TM/ETM+ sensor. According to the above selection scheme, a total of 16 cloud-free images during 1978–2010 were collected from Global Land Cover Facility (<http://glcf.umiacs.umd.edu/data/landsat/>) and Earth Resources Observation (EROS) and Science Center (<http://glovis.usgs.gov/>) (Table 1).

Data preprocessing and other ancillary data

The original Landsat data products were processed systematically, so some preprocessing procedures have to be performed for subsequent analysis of land cover types and change detection. Geometric precision correction, radiometric and atmospheric corrections, image mosaicing and masking were conducted in ENVI (The Environment for Visualizing Images) image processing system. All the images were rectified to WGS 84/UTM zone 50N using a certain number of well-distributed ground control points. The root mean square errors were less than 0.5 pixel (40/15 m) for each of the 16 images. Subsequently, the orthorectification was performed due to the wide coverage of mountain areas in the study area. The products of ASTER GDEM V2 (<http://reverb.echo.nasa.gov/reverb/>) with a spatial resolution of 30 m were used to enhance the image geometry by accounting for the significant spatial distortion caused by relief displacement. To perform the classification and accuracy validation, some reference data were also collected including high-resolution satellite images (e.g., SPOT, QuickBird, Beijing 1), field survey data, and statistical data.

Classification criteria and methods

A classification criterion will be necessary when identifying the land cover types in a certain region. This criterion is required to be more generalized and each specific class could be further divided into more subclasses in accordance with the principal objective and regional land features. Considering the land cover features and available data resources in the study area, a six-class level I classification scheme (Table 2) was specified by referring to the USGS Level I Land Use and Land

Table 1 Captured Landsat time series images during the period 1978–2010

Acquisition date	Path/row	Sensor type	Spatial resolution (m)	Season
June 12, 1978	132/32	Landsat-2 MSS	80	Summer
September 12, 1978	132/32	Landsat-2 MSS	80	Late summer
June 22, 1978	133/32	Landsat-2 MSS	80	Summer
September 20, 1978	133/32	Landsat-2 MSS	80	Late summer
September 7, 1992	123/32	Landsat-5 TM	30	Late summer
September 7, 1992	123/33	Landsat-5 TM	30	Late summer
April 9, 1995	123/32	Landsat-5 TM	30	Spring
April 9, 1995	123/33	Landsat-5 TM	30	Spring
August 2, 1999	123/32	Landsat-7 ETM+	30	Summer
August 2, 1999	123/33	Landsat-7 ETM+	30	Summer
April 30, 2000	123/32	Landsat-7 ETM+	30	Spring
April 30, 2000	123/33	Landsat-7 ETM+	30	Spring
September 20, 2009	123/32	Landsat-5 TM	30	Late summer
September 20, 2009	123/33	Landsat-5 TM	30	Late summer
June 5, 2010	123/32	Landsat-5 TM	30	Summer
June 5, 2010	123/33	Landsat-5 TM	30	Summer

Cover Classification System, which is the most general and allows for land classification at a small scale ($>1: 250,000$), and is used for satellite imagery (Landsat) (Anderson et al. 1976).

After specifying the land cover classification scheme, an effective classification method will be required to identify each class. Traditional supervised and unsupervised classification algorithms have been widely used in previous studies on land use and land cover (Bolstad and Lillesand 1991; Keuchel et al. 2003; Marçal et al. 2005). Nevertheless, most of those methods usually depend on the decision or statistical theories. It is inevitable that mixed pixels and obscure objects will be produced in the process of classification based only on statistical characteristics of spectral values. Conversely, ANN classification algorithms have the capability of improving

automated classification accuracy due to their distributed structure and strong capability of handling complex phenomena, which are relatively unaffected by differences amongst images caused by the atmosphere, illumination, and surface moisture (Sunar Erbek et al. 2004). As a consequence, various kinds of ANN classifiers have recently been explored in remote sensing-based land cover classification (Heerman and Khazenie 1992; Kavzoglu and Mather 2003). In our study, the back-propagation neural network (BPNN) with eigenvector method was used to identify the specified land cover types. To complete the classification process using such a method, five primary steps would be required including preparing available sets of eigenvectors, selecting the optimal combinations of eigenvectors, selecting training sets for each type, designing neural network classifier and setting corresponding parameters, and performing accuracy assessment (Fig. 2).

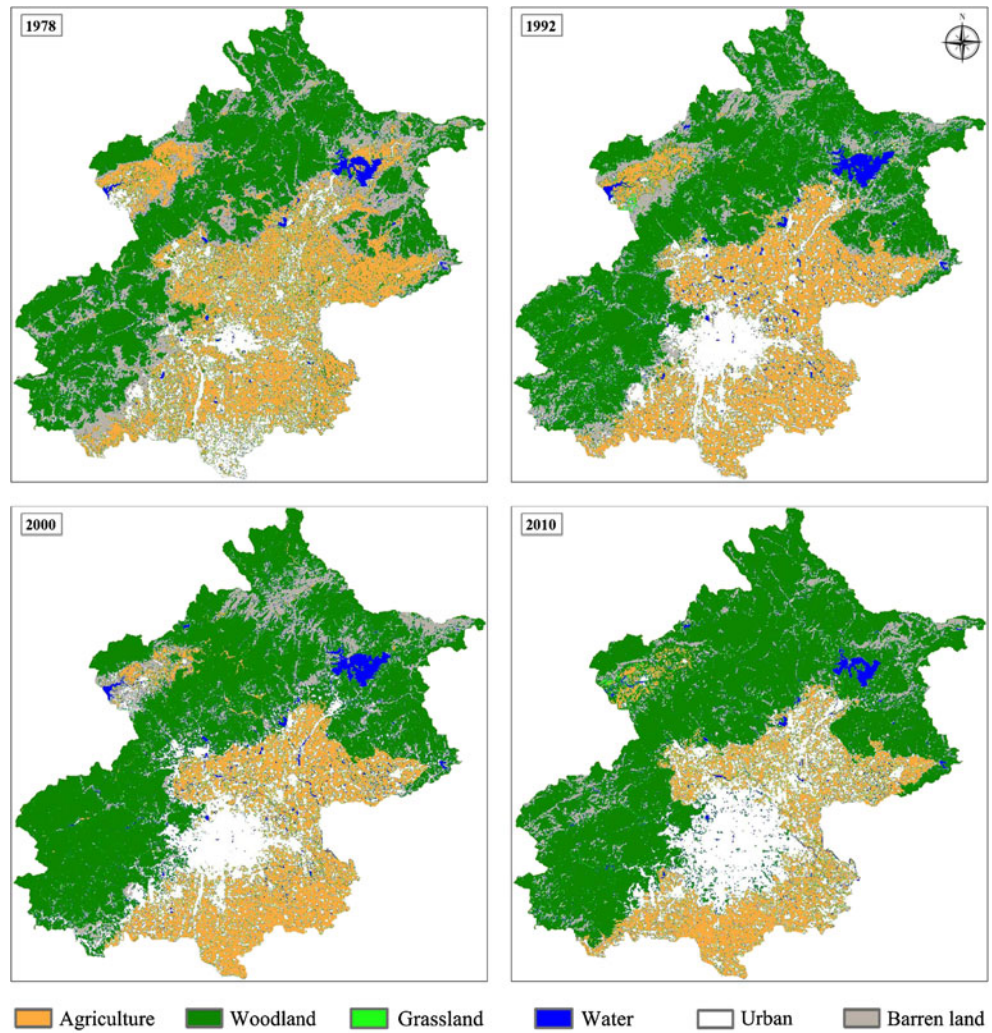
Table 2 Land cover classification scheme

Land cover type	Brief description
Agriculture	Cropland, pasture, and bare or fallow fields
Woodland	Deciduous forest land, evergreen forest land, mixed forest land, orchards, groves, vineyards, and nurseries
Grassland	Golf courses, lawns, and sod fields
Urban	Residential, commercial services, industrial, transportation, communications and utilities, industrial and commercial, mixed urban or build-up land, other urban or built-up land
Water	Permanent open water, lakes, reservoirs, streams, and estuaries
Barren land	Dry salt flats, sandy areas other than beaches, bare exposed rock, strip mines quarries, and gravel pits, transitional areas, and mixed barren land

Land cover change detection

In addition to identifying the land cover types and corresponding amount of each type, it is more important to find out the temporal transitions among different types as they can express the detailed conversion information (Wu et al. 2008). In our study, a multi-date post-classification comparison change detection method was used to determine the changes in land cover in three intervals: 1978–1992, 1992–2000, and 2000–2010 (Jensen 2004). A five-step process will be required to monitor the land cover change in geographic information system (GIS) software: (1) preparing multi-date land cover maps, (2) dissolving data for each map, (3) performing overlaying analysis, (4) identifying the types and acreage of changed regions, and (5) constructing a transition matrix.

Fig. 2 Flowchart for generating land cover map using the neural network with eigenvectors method



Specifically, four maps were firstly generated and incorporated into ArcGIS software environment. Then, the overlaying analysis was carried out to locate sites where these changes occurred. Finally, a transition matrix *A* (Eq. 1) was constructed to find out the magnitude and direction among different land cover types. Based on gains and losses in each category shown by the change matrix, land cover transfer images could be also produced (Zhang et al. 2008). However, it is usually transformed to a cross tabulation for showing quantitative data of the overall land cover changes.

$$A_{ij} = \begin{pmatrix} A_{11} & A_{12} & A_{13} & \dots & A_{1n} \\ A_{21} & A_{22} & A_{23} & \dots & A_{2n} \\ A_{31} & A_{32} & A_{33} & \dots & A_{3n} \\ \dots & \dots & \dots & \dots & \dots \\ A_{n1} & A_{n2} & A_{n3} & \dots & A_{nn} \end{pmatrix} \quad (1)$$

where *n* is the total number of land cover types, *A_{ij}* indicates the total amount of areal changes for a given class *i* (row) to class *j* (column) during the temporal interval of *t* to *t*+1, and both *i* and *j* vary from 1 to *n*.

Additionally, the comprehensive land cover dynamic degree (LCDD) (Zhang et al. 2011) and relative change rate (RCR) (Zhu et al. 2001), derived from the transition matrix, were also calculated to depict the change rate for a certain land cover type (Eqs. 2 and 3).

$$LCDD_T = \left(\frac{\sum_{i=1}^n \Delta LC_{ij}}{\sum_{i=1}^n LC_i} \right) \times 100\% \quad (2)$$

where *LC_i* represents the area of land cover class *i* in the initial time of *t*, ΔLC_{ij} is the change area converted from class *i* to other class *j* (*j*=1, 2, 3, ..., *n*) at the end of time *t*+1.

$$RCR = \frac{|K_b - K_a| \times C_a}{K_a \times |C_b - C_a|} \quad (3)$$

where *K_a* and *K_b* are the area of a certain land cover class between the initial and end time in a local region, and *C_a* and

C_b are the corresponding area of such a class in the entire study area.

Results

Land cover mapping and accuracy assessment

Based on the above classification scheme and algorithm, four land cover maps with six types were generated for 1978, 1992, 2000, and 2010 (Fig. 3). It is obvious that both high- and low-density urban development can be found in the south-central portions of Beijing, while several rural land cover types including agricultural croplands, forests and grasslands characterize the surrounding landscapes. The four maps were the basis for subsequent dynamic change analysis, so it was quite necessary to present their classification accuracies. Confusion matrix was employed to show the accuracy of land cover classification by referring to the ground truth information (Congalton 1991). When selecting the ground truth data, a stratified sampling scheme was used to make sure that reference points or regions of interest (ROIs) could distribute across the study area (Achard et al. 2002). The producer's and users' accuracies were calculated for each type and the overall accuracies were obtained for all the classes (Table 3). Considering the overall accuracies, it could be observed that the classification for 2000 had the highest accuracy, they had the similar accuracies for 1978 and 1992, and

it had the worst accuracy for 2010. Furthermore, they also showed different accuracy differences for six types among four-year maps.

It was obvious that the spatial distribution of each type and the change trends among different years could be visually observed. Considering the spatial distribution, some conclusions could be qualitatively drawn: (1) woodland, agriculture, and urban land were the dominant types, and woodland accounted for almost half of the study area; (2) woodland could be found mainly in the western, eastern and northeastern regions; (3) almost all the agriculture distributed around the urban areas; and (4) Beijing had been undergoing a process of rapid urban sprawl during 1978–2010. Furthermore, the specific area of each type for the four periods were identified (Table 4), according to the analysis of four land cover maps (Fig. 3). Some conclusions could be quantitatively proven and new conclusions could be drawn from Table 4. Woodland and urban types had showed a fast-growing trend; on the contrary, agriculture and barren land had a gradually decreasing trend over the 30 years. Woodland recorded the largest increase relative to the total area, from 40.15 % in 1978 to 54.55 % in 2010, while agriculture had the largest decrease from 29.54 % in 1978 to 17.13 % in 2010. Concerning the grassland and water, they had no significant change trend. When considering the change rate during 1978–2010, agriculture, grassland, and barren land held the negative value to show a decrease trend; on the contrary, woodland, water, and urban land had the positive value to show an increasing trend.

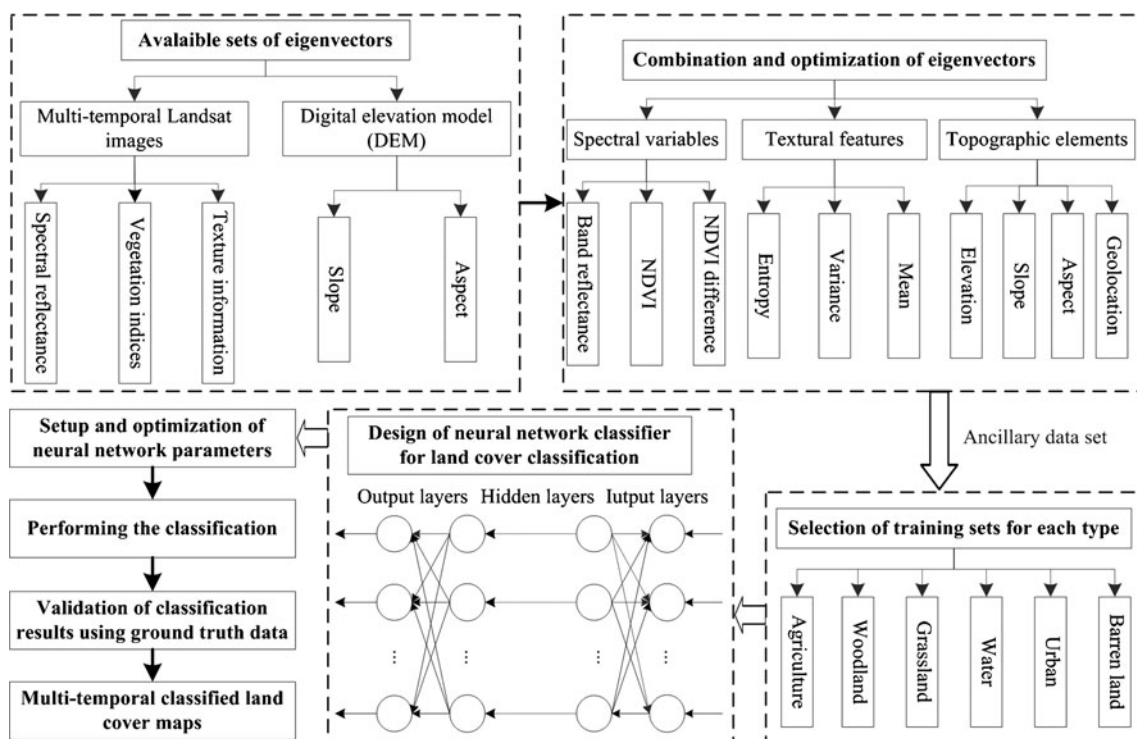


Fig. 3 Land cover maps generated from Landsat time series imagery for 1978, 1992, 2000, and 2010

Table 3 Summary of classification accuracies (in percent) for 1978, 1992, 2000, and 2010 based on the Landsat imagery

Land cover type	1978		1992		2000		2010	
	Producer's	Users'	Producer's	Users'	Producer's	Users'	Producer's	Users'
Agriculture	86.01	88.13	86.68	87.86	86.48	83.14	80.67	74.33
Woodland	85.58	81.11	87.86	83.67	85.18	84.82	85.77	83.37
Grassland	84.17	88.11	81.40	88.04	87.83	87.64	72.38	83.07
Water	87.64	87.74	88.85	88.67	83.20	85.53	86.87	88.52
Urban	88.48	88.37	83.88	88.42	81.72	88.58	81.61	82.86
Barren land	83.42	72.12	86.34	74.97	81.34	83.36	79.04	74.33
Overall accuracy	84.17		84.67		85.35		78.73	

Detection of areal change and transfer direction

Transition matrices were used to monitor both the amount and direction of land cover changes corresponding to the periods 1978–1992, 1992–2000 and 2000–2010 (Table 5). The transitions among different types frequently occurred, but the amount and direction of transfer in and transfer out were extremely different for each type. Considering the change rates among six types, the most dramatic change took place to grassland, barren land, and agriculture, except the water, during the three temporal intervals. Agriculture and barren land showed a net outflow and woodland and urban type had a net inflow. To show the general change intensity of all the types, the comprehensive index of LCDD was used (Fig. 4). It could be seen that the comprehensive change rate showed an increase trend (1992–2010), and it was 38.10 % during 1978–2010.

During the period 1978–1992, agriculture held the largest amount of transfer out (1,928.390 km²), barren land was in the second place (1,301.433 km²), and water had the least amount (25.132 km²). The descending order was agriculture, barren land, urban area, woodland, grassland, and water in light of the areal change. Furthermore, considering the transfer direction among six types, they showed different conditions. Specifically, 1,188.433 km² of the transferred-out agriculture were flown to urban area. Similarly, 481.280 km² of woodland was mainly converted to barren land; 50.378 km² of grassland was primarily transferred to agriculture; and 1,188.494 km² of

barren land was mainly converted to woodland. Considering the amount and direction of transfer in, they differed from transfer out for each land cover type. A total of 1,468.139 km² of woodland were increased and derived mainly from barren land. Urban area was in the second place and the increment was 1,293.266 km², which were mainly derived from agriculture. They were woodland, urban, agriculture, barren land, grass land and water in a descending order, in accordance with the acreage gains.

During the period 1992–2000, agriculture was the primary source of transfer out and 1,134.780 km² were flown to urban area (376.923 km²) and woodland (30.055 km²). The barren land was in the second place and 1,075.578 km² were mainly converted to woodland (480.780 km²) and agriculture (109.797 km²). According to the amount of transfer out, they were agriculture, barren land, woodland, urban, grassland, and water in a descending order. Conversely, woodland had the largest gain and 1,555.228 km² were increased mainly from barren land (979.142 km²) and agriculture (392.665 km²). The urban area was in the second place and 730.745 km² were added mainly from barren land (59.069 km²) and agriculture (577.812 km²). According to the amount of transfer in, they were woodland, urban, barren land, agriculture, water and grassland in a descending order.

Similarly, agriculture and barren land were still the primary source of transfer out during the period 2000–2010. A total of 1,294.541 km² agriculture was primarily transferred to urban

Table 4 Areal and ratio statistics for six-class classification of Beijing during 1978–2010

Year	Agriculture (km ²)	Woodland (km ²)	Grassland (km ²)	Water (km ²)	Urban (km ²)	Barren land (km ²)
1978	4,839.421	6,577.819	123.698	185.316	2,441.885	2,215.641
1992	4,042.992	7,364.763	225.316	370.598	2,617.536	1,762.574
2000	3,383.138	8,341.171	81.251	355.292	2,853.727	1,369.200
2010	2,807.080	8,936.965	50.225	257.573	3,404.734	927.202
Difference ^a	-2,032.341	2,359.146	-73.473	72.257	962.849	-1,288.439
Change rate/%	-42.00	35.87	-59.40	38.99	39.43	-58.15

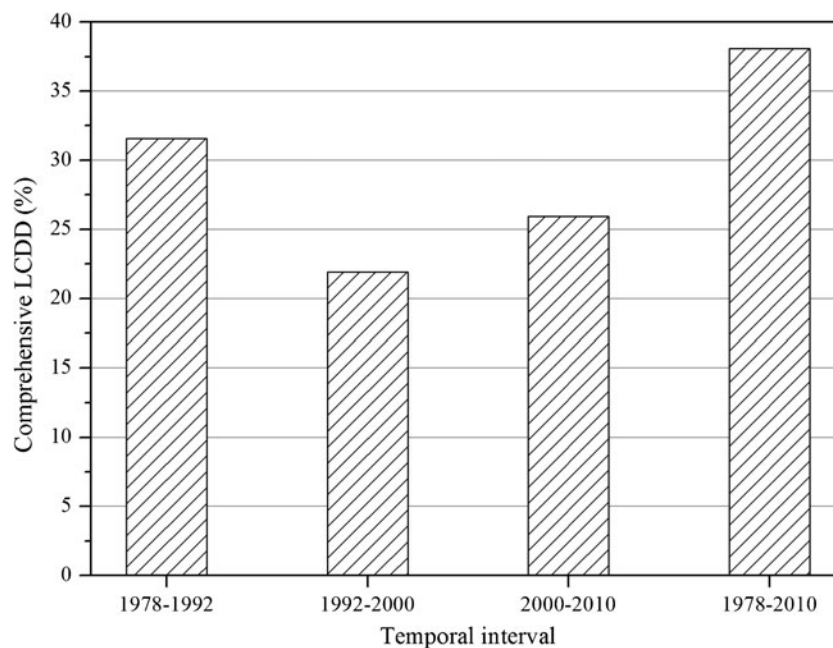
^a Denotes the areal difference of a certain type between the year 1978 and 2010

Table 5 Land cover transition matrices for the six types in the three periods during 1978–2010 (in square kilometer)

1978–1992	Agriculture	Woodland	Grassland	Water	Urban	Barren land	1992	Change rate/%
Agriculture	2,911.031	69.418	50.378	7.672	981.388	23.105	4,042.992	-16.46
Woodland	234.095	5,896.624	30.299	2.438	12.813	1,188.494	7,364.763	11.96
Grassland	66.538	85.084	3.548	0.332	27.856	41.958	225.316	82.15
Water	127.086	12.520	4.885	160.185	49.718	16.205	370.598	99.98
Urban	1,188.433	32.894	26.578	13.689	1,324.270	31.672	2,617.536	7.19
Barren land	312.238	481.280	8.009	1.001	45.840	914.207	1,762.574	-20.45
1978	Agriculture	Woodland	Grassland	Water	Urban	Barren land	2000	Change rate/%
1992	4,839.421	6,577.819	123.698	185.316	2,441.885	2,215.641	16,383.779	
Agriculture	2,908.211	30.055	21.889	27.619	376.923	18.441	3,383.138	-16.32
Woodland	392.665	6,785.943	114.179	15.983	53.259	979.142	8,341.171	13.26
Grassland	15.884	31.277	11.121	1.882	5.742	15.345	81.251	-63.94
Water	38.623	10.234	2.024	278.104	22.726	3.582	355.292	-4.13
Urban	577.812	26.474	28.483	38.907	2,122.982	59.069	2,853.727	9.02
Barren land	109.797	480.780	47.619	8.104	35.904	686.996	1,369.200	-22.32
1992	4,042.992	7,364.763	225.316	370.598	2,617.536	1,762.574	16,383.779	
2000–2010	Agriculture	Woodland	Grassland	Water	Urban	Barren land	2010	Change rate/%
Agriculture	2,088.597	216.357	7.008	38.650	418.002	38.466	2,807.080	-17.03
Woodland	204.441	7,407.481	60.628	82.006	186.223	996.187	8,936.965	7.14
Grassland	14.160	7.433	1.982	2.435	6.423	17.792	50.225	-38.18
Water	24.740	15.437	1.177	174.641	30.556	11.022	257.573	-27.50
Urban	1,033.892	123.392	4.283	50.721	2,177.033	15.413	3,404.734	19.31
Barren land	17.308	576.869	6.173	6.839	35.491	290.319	927.202	-32.28
2000	3,383.138	8,341.171	81.251	355.292	2,853.727	1,369.200	16,383.779	

area (418.002 km²) and woodland (216.357 km²). A total of 1,078.880 km² barren land was primarily transferred to woodland (576.869 km²) and urban area (35.491 km²). The order of

transfer out was agriculture, barren land, woodland, water, urban, and grassland, respectively. Considering the transfer in of each type in 2010, woodland and urban area still obtained

Fig. 4 Comprehensive land cover dynamic degree of the study area during 1978–2010

a lot of transfer in from other types. Specifically, 1,529.484 km² woodland was mainly added from 996.187 km² barren land and 204.441 km² agriculture, and 1,227.702 km² urban area was increased mainly from 1,033.892 km² agriculture and 123.392 km² woodland. Concerned with the amount of transfer in, they were woodland, urban, agriculture, barren land, water, and grassland in a descending order.

Spatial patterns of changed types

After analyzing the changes in amount and transfer direction depending on transition matrices (Table 5), it was more important to investigate the spatial patterns for changed types such as agriculture, urban, woodland, etc. Agriculture was taken as the example to show the spatial characteristics interacting with other types. As shown in Fig. 5, agriculture was primarily converted to urban area and woodland. Spatially, the urban areas converted from agriculture mainly distributed around the central urban areas, including Haidian, Chaoyang, Fengtai, Changping, Daxing, and Shunyi, while the woodland converted from agriculture mainly distributed in

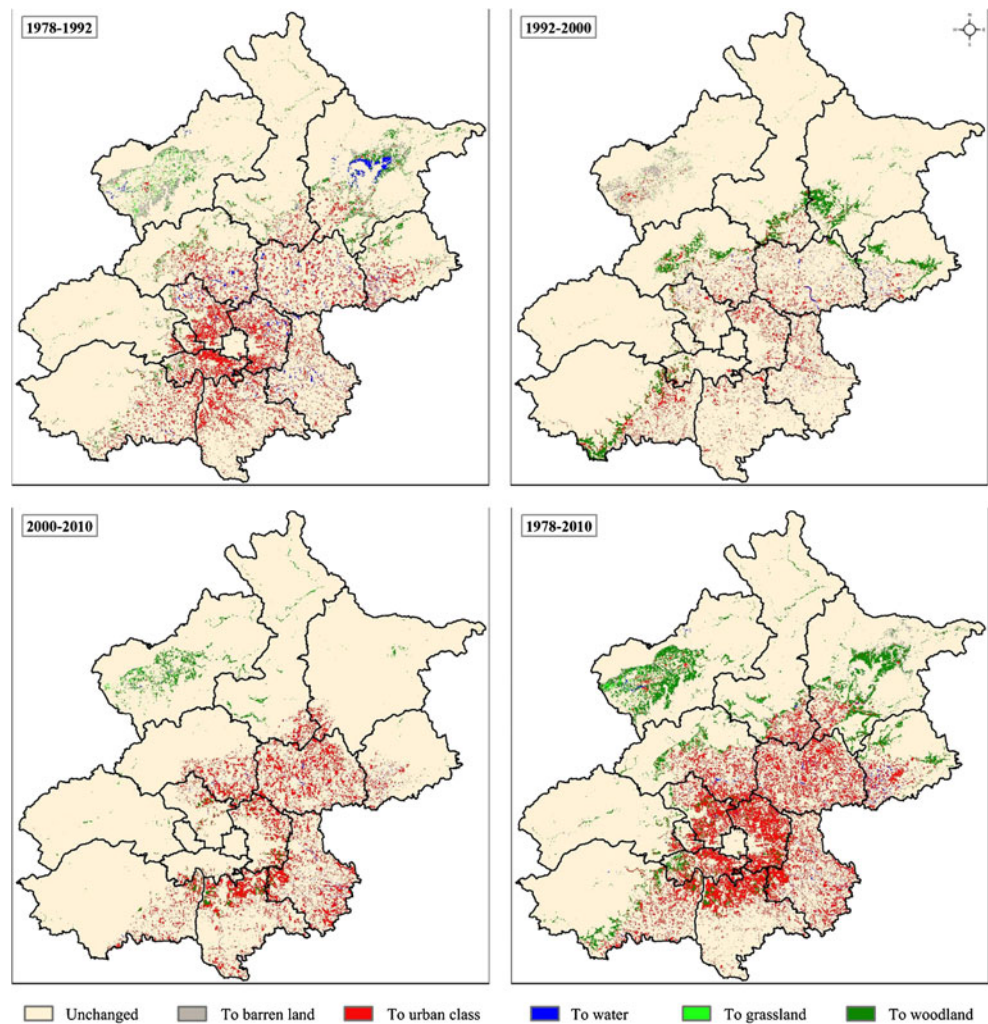
the mountain areas including Yanqing, Miyun, and Pinggu. To compare the RCR for a given type among different hot regions, agriculture was taken as a study case and Chaoyang and Yanqing were used as the study area to comparatively analyze their RCRs (Eq. 3). The result showed that it was 2.2 for Chaoyang and it was 26.1 for Yanqing between 1978 and 2010, which indicated that the RCR of agriculture was larger in Yanqing than in Chaoyang.

Discussion

Analysis of land cover identification and accuracy

Land cover shows a specific landscape with different types for a specific study area, whose amount and spatial distribution can meet a wide variety of spatial needs for human beings. It has been considered as the essential background information in many applications, such as land degradation, rural sustainability, and landscape fragmentation (Mundia and Aniya 2006; Kamusoko et al. 2009; Dewan et al. 2012). Different

Fig. 5 Conversion of agriculture to other land cover types during the period 1978–2010



methods for identifying land cover have experienced significant changes ranging from intensive field sampling with plot inventories to extensive analysis using remotely sensed data (Rogan and Chen 2004). However, land cover does not always keep an unchanging status and can also be obviously changed due to human and natural activities. Actually, there are two primary objectives regarding land cover in an area. One is to identify the land cover types accurately, and the other is to monitor their dynamic changes at a time span. With the development of modern socioeconomic activities, the updating frequency of land cover dynamics has shown a rapid trend. Consequently, identification of land cover information, especially assessing the dynamic changes in fast-growing metropolis (e.g., Beijing, Shanghai, Tianjin, etc.), have been considered as an important parameter for sustainable planning in the context of agriculture, urban development, and nature conservation (Huth et al. 2012). In previous studies, they have been considered as major concerns on how to accurately identify land cover, do dynamic assessment and find out driving forces causing the changes.

Although satellite data with various spatial, temporal, spectral, and radiometric resolutions and different swath widths have been continuously developed, land cover mapping should be considered in relation to requirements, data sources and analysis methodologies (Cihlar 2000; Braimoh and Onishi 2007). The primary goal of this study is to characterize the spatiotemporal dynamics of land cover in Beijing. It is quite important to select appropriate remotely sensed data. Concerning the requirements of spatial and temporal resolutions, Landsat time series imagery was adopted in our study. Nevertheless, there are many difficulties confronting the identification of land cover, due to the complexities and heterogeneities regarding land cover types in metropolis and the resolution constraints on remotely sensed imagery. In previous studies of land cover based on Landsat imagery, spectral information was primarily used (Townshend 1984). Unfortunately, it is inevitable that the phenomenon “the same object with different spectra” and “the same spectrum corresponding to different objects” always occurs among different land cover types. The errors of omission and commission are usually greater, so the classification accuracies are greatly affected. Considering the above disadvantages, multi-seasonal imagery was essential for discriminating confused land cover types (e.g., agriculture and urban area, agriculture, and woodland). Additionally, some new methods were proposed by integrating more ancillary data, such as spatial structural information, topographical parameters and vegetation indices which could greatly reduce spectral confusion and increase the accuracy of land cover classification compared to only spectral classification (Sah et al. 2005; Alfugara et al. 2009). In our study, two things were done to make sure that the classification maps could be more accurate. One was to optimally select the Landsat imagery prior to performing classification. The other

was to adopt the efficient method of neural network with eigenvectors.

Specifically, spring and summer images were primarily selected in accordance with the specific features of defined land cover types. After selecting the images, the neural network classification method was used to identify different types by inputting spectral bands, texture variables, DEM, slope, aspect, normalized difference vegetation index. The overall classification accuracies were 84.17, 84.67, 85.35, and 78.73 for 1978, 1992, 2000, and 2010, respectively (Table 3). It could be seen that it had the highest accuracy for 2000; they were almost the same for 1978 and 1992; and it was lowest for 2010. The differences could be ascribed to the following two aspects: on the one hand, the image quality has been improved from Landsat MSS, TM to etM+, on the other hand, the land cover scenarios have been changing and becoming more fragmented. With the improvement of Landsat imagery from MSS to etM+, the spatial resolutions and available spectral bands were also increased, which greatly improved the spectral separability and heterogeneity among different types. Furthermore, the increasing landscape fragmentation disrupted the land cover integrity, especially for the agriculture and urban area, due to aggravating human-based socioeconomic activities, which made the spatial distribution of different types more discrete. In addition, the number of collected ground truth points or ROIs for accuracy assessment was also an important factor to affect final accuracy (Congalton 1991). In our study, the availability of ground truth reference data was extremely different in four periods, the amount and positions of reference data were also different. Consequently, there was more likely a lack of ground truth data for some types and excessive data for other types.

Dynamic assessment

Urban areas, with the highest population density and aggravating socioeconomic activities, have usually been paid more attention. As the hot spot and sensitive issues, rapid urbanization and urban sprawl have significant impact on conditions of urban ecosystems. It is highly desirable to improve the ability to monitor urban land cover/land use changes. Remote sensing has proven to be a more cost-effective tool in identifying urban land cover for large regions, small site assessment and analysis (Moody and Woodcock 1995). In previous studies, Landsat data were utilized in most urban land cover/land use change monitoring, due to the uniqueness of the dataset as the only long-term digital archive with a medium spatial resolution and relatively consistent spectral and radiometric resolution (Yang et al. 2003). Subsequently, the spatial analysis functions are usually delivered to geographic information system (GIS). Therefore, the combination of satellite remotely sensed data and GIS for land cover, land use and their changes is a key to many diverse applications such as environment,

forestry, hydrology, agriculture, and geology (Mengistu and Salami 2007; Dewan and Yamaguchi 2009b; Zhao et al. 2012). Jat et al. (2008) monitored the urban sprawl of the Ajmer city (situated in Rajasthan State of India), over a period of 25 years (1977–2002), using the statistical classification approaches of the remotely sensed images obtained from various sensors viz. Landsat MSS, TM, ETM+ and IRS LISS-III, and the spatial analysis techniques of GIS. Dewan and Yamaguchi (2009a) evaluated the land use/cover changes and urban expansion in Greater Dhaka, Bangladesh, between 1975 and 2003 using a supervised classification algorithm and the post-classification change detection technique in GIS. In our study, two distinguishing features can be found compared to other related studies: one is the acreage of the study area (the entire Beijing Metropolis) is large, the other is the efficient classification method (the BPNN with eigenvector) is used.

Landsat MSS, TM, and etM+ images have been widely utilized in land cover, especially in the time series analysis, since its successful launch in 1972 (Yang and Lo 2002). In our study, four-date Landsat satellite images for 1978, 1992, 2000 and 2010 were collected and processed for generating land cover maps during the period 1978–2010. Subsequently, the dynamic changes in amount, transfer direction and spatial pattern for each type were identified. Specifically, the acreage of each type was calculated by the number of pixels and the spatial resolution of Landsat images. Then, the transfer directions at three time intervals were assessed by corresponding land cover transition matrices which have often been considered as an effective tool in quantitatively estimating the change within a specific time span (Petit et al. 2001). Based on the transfer matrix of land cover, two aspects can be exposed: one is to reflect the organization structures of different types at the beginning and end of the study period, the other is to demonstrate the transfer direction among different types. Although a certain land cover type can be theoretically converted to any other types or increased from other types, some transitions cannot usually occur in practical applications. For example, it is normal that agriculture is converted to urban area, but it is always impossible in inverse case. There are few areas where certain categories such as water also transformed to woodland concerning this study. Two reasons can be used to interpret the phenomenon: one is the influence of misclassification because of mixed pixels on different spatial resolution images; the other is the seasonal differences of Landsat images in different years. In addition, it is also difficult to acquire the satellite images or photographs for the study site at constant time intervals. When comparing the transition matrices for different observation periods, they must be normalized at the same observation interval (Takada et al. 2010).

After analyzing the changes in the amount and transfer direction, it is quite necessary to find out the hot regions where the intensities of land cover change are highest. The

comprehensive LCDD and RCR were considered as the two appropriate indices to describe the changes in spatial patterns (Yan et al. 2002), and they were used to depict the change rate for a certain land cover type in our study. It is obvious that the combination of remote sensing and GIS has provided an inexpensive and effective approach for monitoring land cover and its changes. However, for governmental decision-makers, it is just the major concern on how to find out the driving factors and providing a solution for sustainable exploration and protection of precious land resources.

Driving forces analysis

Driving forces analysis is a way of understanding and accounting for land cover changes potentially caused by different factors such as regional climate change, physical and ecological constraints, socioeconomic and political influences, etc. (Serra et al. 2008). Environmental factors, such as slope, aspect, elevation, temperature, precipitation, etc., usually determine the vegetation growth and agricultural development in the fragile ecosystem (Wang et al. 2006). However, in comparison with the constraints of natural conditions, demographic and economic development is the highly basic driving factors in fast-growing metropolitan areas (Lin and Ho, 2003). Typical limiting factors include the rapid population growth, the fast-growing urban and suburban economies, the higher urbanization level, changing institutional policies, etc. Those factors have substantially exerted a significant influence on land cover scenarios in Beijing, especially since Chinese reform and opening up in 1978.

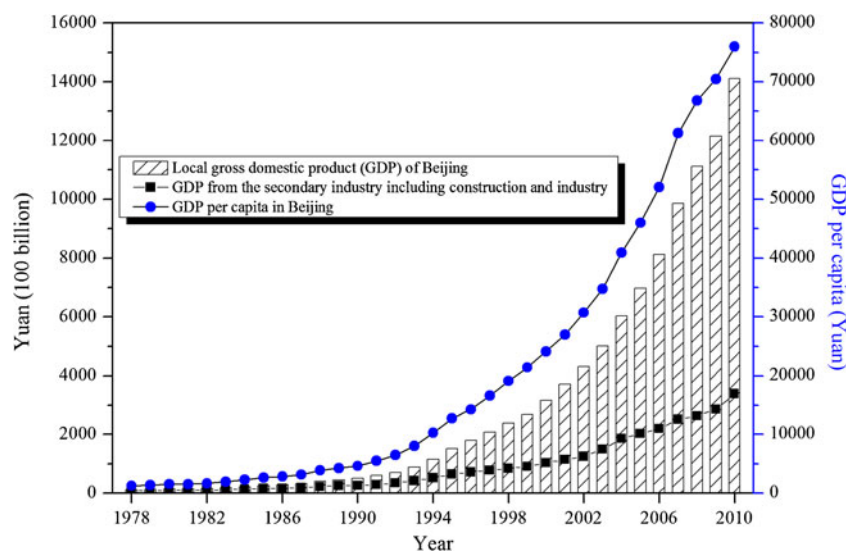
(1) Economic development

As a matter of fact, the urban sprawl and land cover changes are substantially driven by the urgent requirements of social and economic development (Walker 2001). During the period from 1978 to 2010, Beijing has experienced a remarkable period of rapid economic growth spanning more than 30 years (Fig. 6). In 1978, the local gross domestic product (GDP) was just 108.8 (100 billion) Yuan, but it had increased to 500.8, 3,161.7, and 14,113.6 (100 billion) Yuan in 1990, 2000, and 2010, respectively. Similarly, the GDP per capita also showed a rapid growth trend, and it was 1,257, 4,635, 24,127, and 75,943 Yuan in 1978, 1990, 2000, and 2010, respectively. In more than 30 years, the GDP in Beijing increased by 12,872 % and the GDP per capita increased by 5,942 %. It was inevitable that the phenomena of population growth, urban sprawl, reduction of land resources, etc. would occur along with the improvement in economic development (Meyer and Turner II 1992).

(2) Growth of population and construction areas

Since the 1980s, the urban and floating population have experienced a continuous growth, so the total population

Fig. 6 Economic development in Beijing during the period 1978–2010



showed a sharp increase from 871.5 (10,000) in 1978 to 1,961.9 (10,000) in 2010 (Fig. 7a). According to the population statistics from Beijing Statistical Information Net (<http://www.bjstats.gov.cn>), there were totally 19.612 million registered permanent residents in 2010 from the sixth national population census, Beijing. A total of 6.043 million (44.5 %) was increased in 10 years and the average increase was 0.604 million (about 3.8 %) per year compared to the fifth population census in 2000. There are two reasons for such a population growth during the study period. One is that the birth rate and the rate of natural increase per 1,000 population have always kept relatively high values, but the death rate has shown a gradual downward trend (Fig. 7b). The other is that large floating population from 21.8 (10,000) in 1978 to 704.7 (10,000) in 2010, continually enter this metropolis, due to the rapid urbanization and accelerated development in Beijing. Consequently, more and more houses and traffic facilities will be required along with the population growth. According to

the Beijing Statistical Yearbook 2011, the construction areas, the mileages of roads and the number of bridges, have significantly increased from 1978 to 2010. Specifically, the total housing construction area was just 956.3 (10,000 m²) in 1978, but it had reached 15,572.1 (10,000 m²) in 2010 (Fig. 8a). About half of the housing construction areas were used for residential construction. Similarly, the mileage of the roads and streets and the number of bridges have also kept an increasing trend in Beijing during the study period. The total mileage of roads was just 6,562 km in 1978, but it had reached 21,114 km in 2010; the number of bridges was just 351 in 1978, but it was 1,855 in 2010 (Fig. 8b).

(3) Institutional policies

In addition to rapid economic development and population growth, the land cover scenarios are also greatly altered by institutional policies from local or national governments. For example, the Program for Conversion of Cropland to Forests

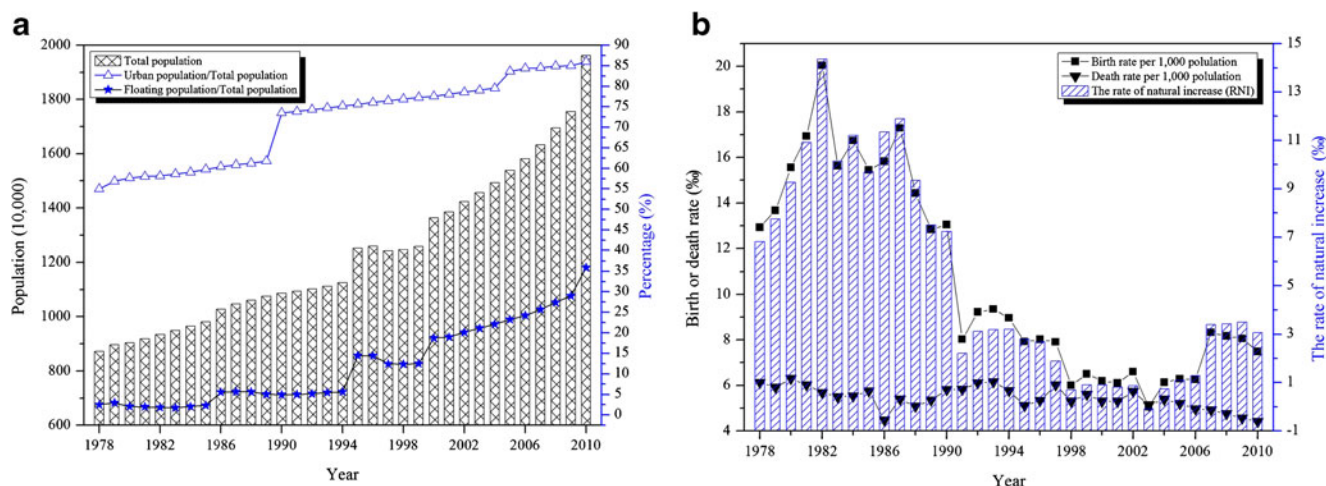


Fig. 7 a Changes of population in Beijing during 1978–2010; b changes of the rates of birth, death and natural increase in Beijing during 1978–2010

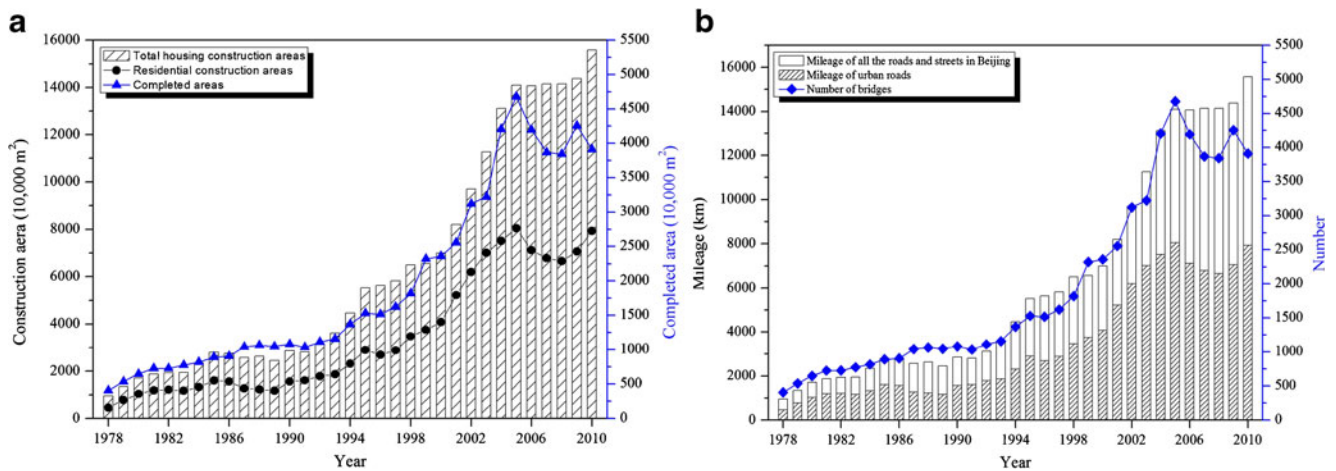


Fig. 8 a Areal changes of housing construction in Beijing during 1978–2010; b changes of the mileage of roads and the number of bridges in Beijing during 1978–2010

was implemented in Beijing in 2000. To reduce or control water and soil loss, barren land and sloping farmland were changed to woodland, especially in mountain areas such as Pinggu District, Huairou District, Yanqing County. It was reported that a total of about 300 km² of farmland have been changed to woodland during 2000–2004. For another example, Beijing's overall planning schemes were specified in different developmental stages. During the period 1991–2000, the strategy was proposed that the metropolitan development gradually transferred from urban to suburban areas, according to the requirements of the socioeconomic development and the amount of urban and floating population. In the updated overall planning schemes (2004–2020), some new plans are also made to determine the spatial patterns in urban landscape to a great degree.

Conclusions

Beijing, a fast-growing and dynamically changing metropolis, was selected as the study area and the land cover and its change were qualitatively and quantitatively characterized by combining remote sensing and GIS spatial analysis techniques during the period 1978–2010. The results showed that Beijing witnessed a dramatic change in land cover over the study period. It experienced a heavy loss in agriculture, grassland and barren land, but had a gain in woodland and urban area. Agriculture decreased from 4,839.421 km² in 1978 to 2,807.080 km² in 2010, on the contrary, urban area increased from 2,441.885 to 3,404.734 km² within the period. Concerned with the transfer direction, agriculture was primarily flown to urban area and woodland. Barren land was mainly converted to woodland and agriculture. Spatially, the urban area converted from agriculture mainly distributed around the central urban areas including Haidian, Chaoyang, Fengtai, Changping, Daxing, and Shunyi, while the woodland

converted from agriculture mainly distributed in the mountain areas including Yanqing, Miyun, and Pinggu. Furthermore, the relationship between land cover dynamics and driving forces was examined. In comparison with environmental constraints, socioeconomic and sociopolitical aspects were just the leading factors to change its land cover in fast-growing Beijing.

To find out the causes of land cover in Beijing, three types of driving factors were primarily discussed including the economic development, growth of population and construction areas, and institutional policies. It was shown that the economy, population, and construction areas had experienced a sharp increase. In more than 30 years, the GDP increased by 12872 % and the GDP per capita increased by 5942 %; the total population increased from 871.5 (10,000) in 1978 to 1,961.9 (10,000) in 2010; the total housing construction area increased from 956.3 (10,000 m²) in 1978 to 15,572.1 (10,000 m²) in 2010; the total mileage of roads increased from 6,562 km in 1978 to 21,114 km in 2010; and the number of bridges increased from 351 in 1978 to 1,855 in 2010. Additionally, institutional policies implemented by local or national governments were also found to affect the spatial patterns in land cover landscape. Based on the above analysis, it can be seen that the combination of remote sensing and GIS techniques is a useful monitoring system to identify spatially land cover types and assess the changes over long time spans in densely populated urban areas. Additionally, the analysis between land cover and some its causative factors are also useful for managing and exploring precious land resources by specifying rational urban planning policies.

Acknowledgments The work presented here was supported by the Beijing Postdoctoral Research Foundation (2012ZZ-84), the Special Support by China Postdoctoral Science Foundation (2013T60080 and 2013T60189), the National Natural Science Foundation of China (41201422 and 41271412), and the Anhui Provincial-Level High School Science Research Project (KJ2013A026).

References

- Achard F, Eva HD, Stibig HJ (2002) Determination of deforestation rates of the world's humid tropical forests. *Science* 297:999–1002
- AlFugara AM, Pradhan B, Mohamed TA (2009) Improvement of land-use classification using object-oriented and fuzzy logic approach. *Appl Geomat* 4(1):111–120
- Al-shalabi M, Billa L, Pradhan B, Mansor S (2013) Modeling urban growth evolution and land-use changes using GIS based Cellular Automata and SLEUTH models: The case of Sana'a metropolitan city. *Yemen Environ Earth Sci*. doi:10.1007/s12665-012-2137-6
- Al-shalabi M, Pradhan B, Billa L, Mansor S (2012) Manifestation of remote sensing data in modeling urban growth pattern using the Sleuth model and Brute Force calibration: a case study of Sana'a City Yemen. *J Indian Soc Remote Sens*. doi:10.1007/s12524-012-0215-6
- Anderson JR, Hardy EE, Roach JT, Richard EW (1976) A land use and land cover classification system for use with remote sensing data. Reston, Virginia' U.S. Geological Survey; USGS professional paper 964, pp 138–145
- Biro K, Pradhan B, Buchroithner MF, Makeshin F (2013) An assessment of land use/land-cover change impacts on soil properties in the northern part of Gadarif region, Sudan. *Land Degrad Dev* 24(1):90–102
- Bolstad PV, Lillesand TD (1991) Rapid maximum likelihood classification. *Photogramm Eng Rem S* 57(1):67–74
- Braimoh AK, Onishi T (2007) Spatial determinants of urban land use change in Lagos, Nigeria. *Land Use Policy* 24(2):502–515
- Cihlar J (2000) Land cover mapping of large areas from satellites: status and research priorities. *Int J Remote Sens* 21:1093–1114
- Congalton RG (1991) A review of assessing the accuracy of classifications of remotely sensed data. *Remote Sens Environ* 37(1):35–46
- DeFries RS, Townshend JRG (1994) Global land cover: comparison of ground based data sets to classifications with AVHRR data. In: Foody G, Curran P (eds) *Environmental remote sensing from regional to global scales*, 1st edn. Wiley, Chichester, p 238
- Dewan AM, Yamaguchi Y (2009a) Land use and land cover change in Greater Dhaka, Bangladesh: using remote sensing to promote sustainable urbanization. *Appl Geogr* 29(3):390–401
- Dewan AM, Yamaguchi Y (2009b) Using remote sensing and GIS to detect and monitor land use and land cover change in Dhaka Metropolitan of Bangladesh during 1960–2005. *Environ Monit Assess* 150(1–4):237–249
- Dewan AM, Yamaguchi Y, Rahman MZ (2012) Dynamics of land use/cover changes and the analysis of landscape fragmentation in Dhaka Metropolitan, Bangladesh. *GeoJournal* 77(3):315–330
- Feddema JJ, Oleson KW, Bonan GB et al (2005) The importance of land-cover change in simulating future climates. *Science* 310:1674–1678
- Flamenco-Sandoval A, Ramos MM, Masera OR (2007) Assessing implications of land-use and land-cover change dynamics for conservation of a highly diverse tropical rain forest. *Biol Conserv* 138(1–2):131–145
- Haack B, Bryant N, Adams S (1987) An assessment of Landsat MSS and TM data for urban and near-urban land-cover digital classification. *Remote Sens Environ* 21(2):201–213
- Heeman PD, Khazenie N (1992) Classification of multispectral remote sensing data using a back-propagation neural network. *IEEE Trans Geosci Remote Sens* 30(1):81–88
- Huth J, Kuenzer C, Wehrmann T (2012) Land cover and land use classification with TWOPAC: towards automated processing for pixel- and object-based image classification. *Remote Sens* 4(9):2530–2553
- Jat MK, Garg PK, Khare D (2008) Monitoring and modeling of urban sprawl using remote sensing and GIS techniques. *Int J Appl Earth Obs* 10(1):26–43
- Jensen JR (2004) *Introductory digital image processing: a remote sensing perspective*, 2nd edn. Prentice-Hall, New Jersey, pp 467–494
- Kamusoko C, Aniya M, Adi B, Manjoro M (2009) Rural sustainability under threat in Zimbabwe—simulation of future land use/cover changes in the Bindura district based on the Markov-cellular automata model. *Appl Geogr* 29(3):435–447
- Kavzoglu T, Mather PM (2003) The use of backpropagating artificial neural networks in land cover classification. *Int J Remote Sens* 24(23):4907–4938
- Kelarestaghi A, Jeloudar ZJ (2011) Land use/cover change and driving force analyses in parts of northern Iran using RS and GIS techniques. *Arab J Geosci* 4(3–4):401–411
- Keuchel J, Naumann S, Heiler M (2003) Automatic land cover analysis for Tenerife by supervised classification using remotely sensed data. *Remote Sens Environ* 86(4):530–541
- Lambin EF, Geist HJ, Lepers E (2003) Dynamics of land-use and land cover change in tropical regions. *Annu Rev Environ Resour* 28(1):205–241
- Lambin EF, Strahler AH (1994) Indicators of land-cover change for change-vector analysis in multitemporal space at coarse spatial scales. *Int J Remote Sens* 15(10):2099–2119
- Lin GCS, Ho SPS (2003) China's land resources and land-use change: insights from the 1996 land survey. *Land Use Policy* 20(2):87–107
- Loveland TR, Reed BC, Brown JF et al (2000) Development of a global land cover characteristics database and IGBP DISCover from 1 km AVHRR data. *Int J Remote Sens* 21(6–7):1303–1330
- Marçal ARS, Borges JS, Gomes JA et al (2005) Land cover update by supervised classification of segmented ASTER images. *Int J Remote Sens* 26(7):1347–1362
- Matinfar HR, Alavi Panah SK, Zand F, Khodaei K (2013) Detection of soil salinity changes and mapping land cover types based upon remotely sensed data. *Arab J Geosci* 6(3):913–919
- Mengistu DA, Salami AT (2007) Application of remote sensing and GIS inland use/land cover mapping and change detection in a part of south western Nigeria. *Afri J Environ Sci Technol* 1(5):99–109
- Meyer WB, Turner BL II (1992) Human population growth and global land-use/cover change. *Annu Rev Ecol Systemat* 23(1):39–61
- Moody A, Woodcock CE (1995) The influence of scale and the spatial characteristics of landscapes on land-cover mapping using remote sensing. *Landscape Ecol* 10(6):363–379
- Mundia CN, Aniya M (2006) Dynamics of land use/cover changes and degradation of Nairobi City, Kenya. *Land Degrad Dev* 17(1):97–108
- Oettera DR, Cohenb WB, Berterretchea M et al (2000) Land cover mapping in an agricultural setting using multiseasonal Thematic Mapper data. *Remote Sens Environ* 76(2):139–155
- Petit C, Scudder T, Lambin E (2001) Quantifying processes of land-cover change by remote sensing: Resettlement and rapid land-cover changes in south-eastern Zambia. *Int J Remote Sens* 22(17):3435–3456
- Ramankutty N, Foley JA (1999) Estimating historical changes in global land cover: croplands from 1700 to 1992. *Global Biogeochem Cycles* 13(4):997–1027
- Rogan J, Chen DM (2004) Remote sensing technology for mapping and monitoring land-cover and land-use change. *Prog Plann* 61(4):301–325
- Rogan J, Miller J, Stow D et al (2003) Land-cover change monitoring with classification trees using Landsat TM and ancillary data. *Photogramm Eng Rem S* 69(7):793–804
- Sah AK, Arora MK, Csaplovics E (2005) Land cover classification using IRS LISS III image and DEM in a rugged terrain: a case study in Himalayas. *Geocarto Int* 20(2):33–40
- Serra P, Pons X, Sauri D (2008) Land-cover and land-use change in a Mediterranean landscape: a spatial analysis of driving forces integrating biophysical and human factors. *Appl Geogr* 28(3):189–209
- Sobrino JA, Raissouni N (2000) Toward remote sensing methods for land cover dynamic monitoring: application to Morocco. *Int J Remote Sens* 21(2):353–366

- Stathopoulou M, Cartalis C (2007) Daytime urban heat islands from Landsat etM+ and Corine land cover data: an application to major cities in Greece. *Sol Energy* 81(3):358–368
- Stone TA, Schlesinger P, Houghton RA et al (1994) A map of the vegetation of South America based on satellite imagery. *Photogramm Eng Rem S* 60(5):541–551
- Sunar Erbek F, Özkan C, Taberner M (2004) Comparison of maximum likelihood classification method with supervised artificial neural network algorithms for land use activities. *Int J Remote Sens* 25(9):1748–1773
- Takada T, Miyamoto A, Hasegawa SF (2010) Derivation of a yearly transition probability matrix for land-use dynamics and its applications. *Landscape Ecol* 25(4):561–572
- Tehrany MS, Pradhan B, Jebur MN (2013) Remote sensing data reveals eco-environmental changes in urban areas of Klang Valley Malaysia: contribution from object based analysis. *J Indian Soc Remote Sens*. doi:10.1007/s12524-013-0289-9
- Townshend JRG (1984) Agricultural land-cover discrimination using thematic mapper spectral bands. *Int J Remote Sens* 5(4):681–698
- Turner BL II, Meyer WB, Skole DL (1994) Global land-use/land-cover change: towards an integrated study. *Ambio* 23(1):91–95
- Walker R (2001) Urban sprawl and natural areas encroachment: linking land cover change and economic development in the Florida Everglades. *Ecol Econ* 37(3):357–369
- Wang GX, Wang YB, Kubota J (2006) Land-cover changes and its impacts on ecological variables in the headwaters area of the Yangtze River, China. *Environ Monit Assess* 120(1–3):361–385
- Wu X, Shen ZY, Liu RM et al (2008) Land use/cover dynamics in response to changes in environmental and socio-political forces in the upper reaches of the Yangtze River, China. *Sensors* 8(12):8104–8122
- Yan JZ, Zhang YL, Liu LS et al (2002) Land use and landscape pattern change: a linkage to the construction of the Qinghai-Xizang Highway. *J Geogr Sci* 12(3):253–265
- Yang L, Xian G, Klaver JM, Deal B (2003) Urban land-cover change detection through sub-pixel imperviousness mapping using remotely sensed data. *Photogramm Eng Rem S* 69(9):1003–1010
- Yang X, Lo CP (2002) Using a time series of satellite imagery to detect land use and land cover changes in the Atlanta, Georgia metropolitan area. *Int J Remote Sens* 23(9):1775–1798
- Youssef AM, Pradhan B, Tarabees E (2011) Integrated evaluation of urban development suitability based on remote sensing and GIS techniques: contribution from the analytic hierarchy process. *Arab J Geosci* 4(3–4):463–473
- Yuan F, Bauer ME, Heinert N et al (2005a) Multi-level land cover mapping of the Twin Cities (Minnesota) Metropolitan Area with multi-seasonal Landsat TM/ETM+ data. *Geocarto Int* 20(2):5–14
- Yuan F, Sawaya KE, Loeffelholz et al (2005b) Land cover classification and change analysis of the Twin Cities (Minnesota) Metropolitan Area by multitemporal Landsat remote sensing. *Remote Sens Environ* 98(2–3):317–328
- Zhang H, Wang X, Ho HH et al (2008) Eco-health evaluation for the Shanghai metropolitan area during the recent industrial transformation (1990–2003). *J Environ Manage* 88(4):1047–1055
- Zhang H, Zhou LG, Chen MN et al (2011) Land use dynamics of the fast-growing Shanghai Metropolis, China (1979–2008) and its implications for land use and urban planning policy. *Sensors* 11(2):1794–1809
- Zhao JL, Xue YA, Yang H et al (2012) Evaluating and classifying field-scale soil nutrient status in Beijing using 3S technology. *Int J Agric Biol* 14(5):689–696
- Zhu HY, Li XB, He SJ et al (2001) Spatial-temporal change of land use in Bohai Rim. *Acta Geograph Sin* 56(3):253–260 (in Chinese)